LIP-STUDENTS-25-21

High-precision fully differential predictions for top-pair production at the LHC in perturbative QCD

Duarte Barreta[1,a]

[1] *Faculdade de Ciências da Faculdade da Universidade de Lisboa*

Project supervisor: João Pires

October 29, 2025

Abstract. This paper aims to study the differential cross sections for the production of topantitop pairs from protonproton collisions at the LHC within the framework of perturbative QCD. The software fastNLO was used to perform the calculations related to top-pair production, and the evaluation was extended to the Next-to-Next-to-Leading-Order.

KEYWORDS: LHC, top-pair, perturbative QCD

1 Introduction

1.1 The top-pair production

The LHC is a big factory of many particles, as is the case with the pair of top and anti-top quarks. For the production of this particle pair, it is important to note that they originate from protonproton collisions, with each proton composed of two up quarks and one down quark. These quarks form a bound state held together by the strong force, mediated by gluons. Furthermore, gluons can split into quarkantiquark pairs through quantum fluctuations. These $q\bar{q}$ pairs can then participate in the hard scattering processes that produce topantitop ($t\bar{t}$) pairs. The most significant contributions come from up and down quark pairs, since protons are composed of two up quarks and one down quark (uud).

In the following Feynman Diagram, we can see the illustration of the process described:

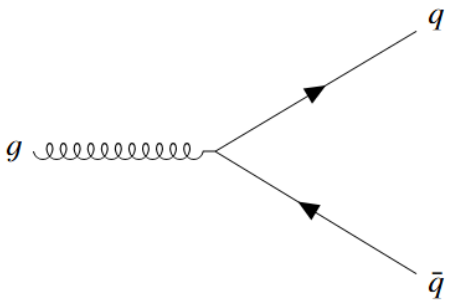

Figure 1: Production of a pair of $q\bar{q}$ from a gluon.

The production of topantitop pairs occurs during protonproton collisions, which require a sufficiently high partonic center-of-mass energy - roughly twice the top quark mass. In this study, collisions at center-of-mass energies of 8 TeV and 13 TeV were considered, well above this threshold. Once a quark from one proton collides with an antiquark of the same flavor from the other proton, $t\bar{t}$ production can occur via $q\bar{q}$ annihilation. In addition, gluongluon fusion processes can also contribute, as shown in the Feynman diagrams in Figure 2.

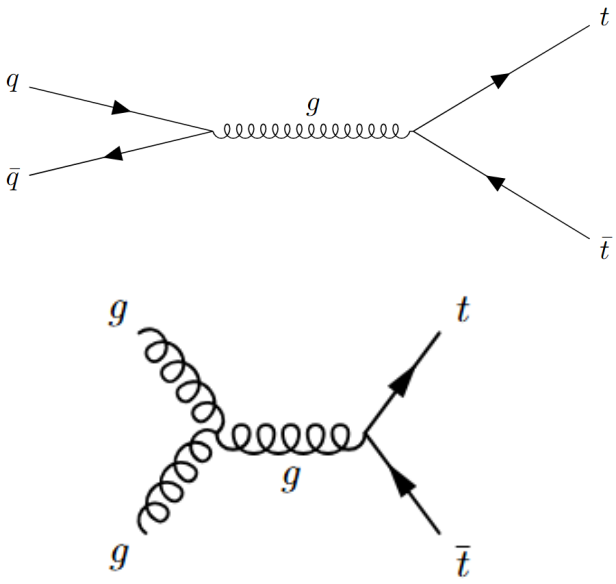

Figure 2: Production of the pair $t\bar{t}$ from a pair $q\bar{q}$ and from 2 gluons.

1.2 My work on the internship

My work in this internship was developed with the fastNLO software [1]. It was also necessary to use parton distribution functions (PDFs [2]) and the fastNLO tables for topantitop production [3] to predict the differential cross section for $t\bar{t}$ production at the LHC.

The predictions considered in this study were made for 4 observables: M_{tt}, Y_{tt}, Y_{avt}, and P_{tavt}. These observables stand for:

- $M_{t\bar{t}}$: Invariant Mass

$$M_{t\bar{t}} = (p_t + p_{\bar{t}})$$

[a] e-mail: duartebarreta@gmail.com

- $Y_{t\bar{t}}$: Rapidity of the top-antitop pair

$$Y_{t\bar{t}} = \frac{1}{2}\ln\left(\frac{E+p_z}{E-p_z}\right)$$

- Y_{avt}: Average Rapidity of the top-antitop pair

$$Y_{avt} = \frac{1}{2}(y_t + y_{\bar{t}})$$

- $P_{T,avt}$: Average top-antitop transverse momentum

$$P_{T,avt} = \frac{1}{2}(p_T^t + p_T^{\bar{t}})$$

For all predictions generated in this study, two sources of uncertainty were considered: the variation of the renormalization scale (μ_R) and the variation of the parton distribution functions (PDFs). The PDF describes the probability of finding a parton (quark, antiquark, or gluon) inside a fast-moving hadron and the renromalization scale, μ_R, sets the energy scale at which the strong coupling constant α_s is evaluated.

Also, it is important to say that the results were given in function of terms of the perturbative QCD expansion, where the first 3 terms were considered:

- LO (Leading Order): this is the first term of the perturbative expansion
- NLO (Next to Leading Order):
- NNLO (Next to Next to Leading Order)

2 Evaluation of the convergence of the perturbative expansion

In the first place, it was used the *fastNLO* software to calculate the differential cross sections for the observables mentioned in the previous section for proton-proton collisions at 13TeV for the PDF NNPDF30. We set the renormalization scale equal to factorization scale and equal to the top quark mass $\mu_R = \mu_F = m_t$ with $m_t = 173.3\ GeV$. The next step was plotting on a histogram the 3 orders of the perturbative expansion in analysis to verify if the series converges. This is shown in Figure 3 and Figure 4.

In the subplot of each figure, the K-factors are shown, which quantify the relative change between successive perturbative terms. They are defined as:

$$KNLO = \frac{NLO}{LO} \qquad KNNLO = \frac{NNLO}{NLO}$$

And we can note that for all the observables, $KNLO$ tells us that on average there is a growth of almost 40% from LO to NLO and only a growth of around 10% from NLO to NNLO, which means that the series converges.

3 Estimation of theoretical uncertainties

3.1 Variation of the renormalization scale

To estimate the uncertainty due to the variation of the renormalization scale, the differential cross section at

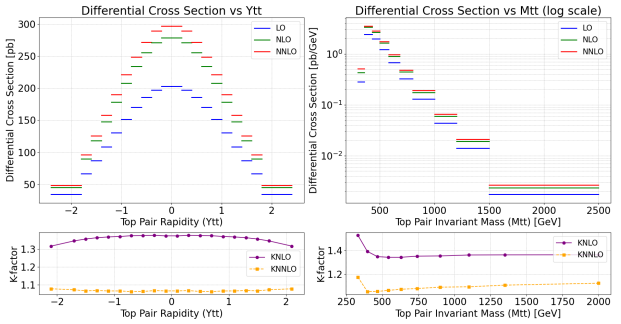

Figure 3: Histogram of the Differential Cross Section in function of $Y_{t\bar{t}}$ and $M_{t\bar{t}}$ for LO, NLO, and NNLO at $\sqrt{s} = 13\ TeV$.

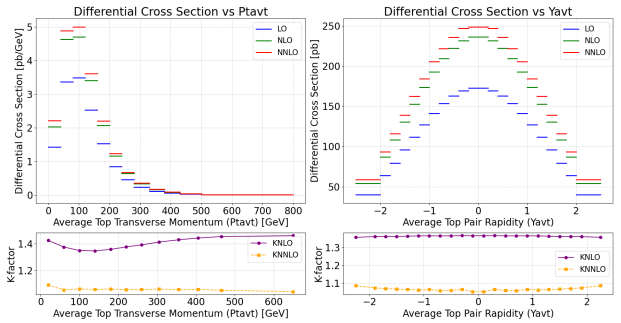

Figure 4: Histogram of the Differential Cross Section in function of $P_{T,avt}$ and Y_{avt} for LO, NLO, and NNLO at $\sqrt{s} = 13\ TeV$.

13 TeV was computed using the NNPDF30 set with μ_R varied by factors of 2 and 0.5. The results are shown in Figures 5,6 and 7.

As can be seen, at Leading Order (LO) there is a significant difference in the cross section when varying μ_R: on average, $\mu_R = 0.5$ leads to an increase of about 24%, while $\mu_R = 2$ results in a decrease of approximately 33%. The effect is therefore quite dramatic.

At Next-to-Leading Order (NLO), the differences are smaller: for $\mu_R = 0.5$, a variation of about 8% is observed, while for $\mu_R = 2$, the variation is approximately 15%.

Finally, at Next to Next to Leading Order (NNLO), the deviation increases again, approximately 11% for $\mu_R = 0.5$ and 19% for $\mu_R = 2$. This behavior is unexpected, as the deviation is generally expected to decrease with increasing perturbative order. The observed trend most likely arises from limitations in the interpolation grid table provided in Ref. [3], which may not contain all the ingredients required to perform a proper scale variation at this order. Therefore, further studies using Monte Carlo simulations are required to fully evaluate this situation.

3.2 PDF uncertainty

To estimate the PDF uncertainty in the differential cross section, predictions were generated using several PDF sets

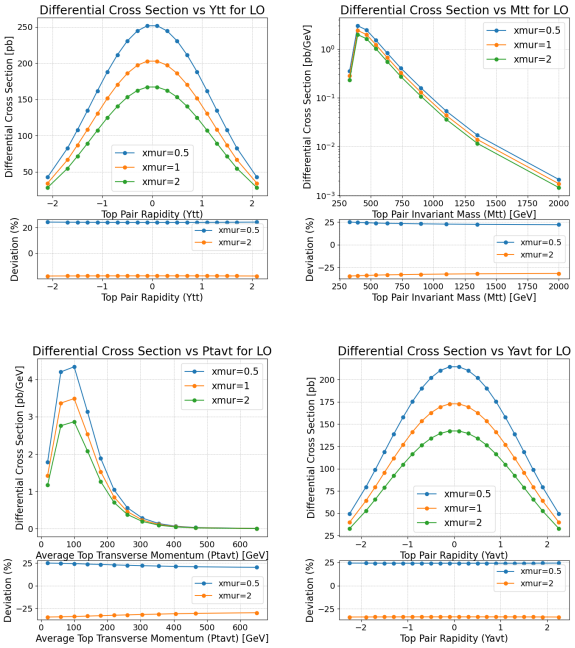

Figure 5: Plot of the Differential Cross Section (LO) as a function of the observables for 3 values of μ_R and the deviation from $\mu_R = 1$.

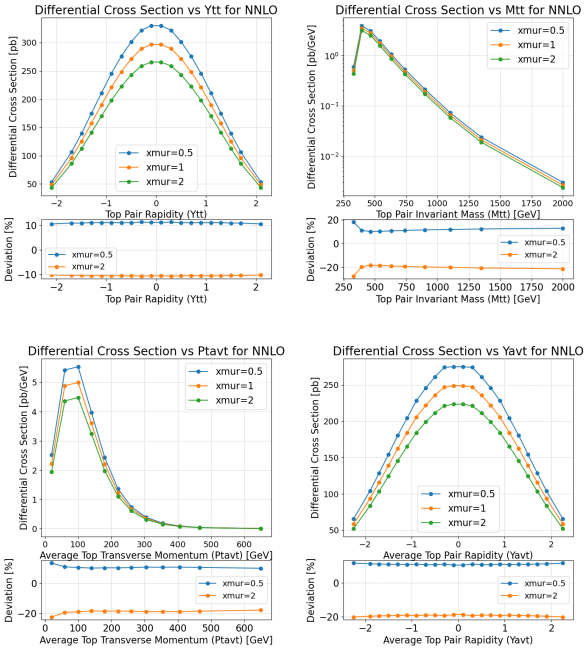

Figure 7: Plot of the Differential Cross Section (NNLO) as a function of the observables for 3 values of μ_R and the deviation from $\mu_R = 1$.

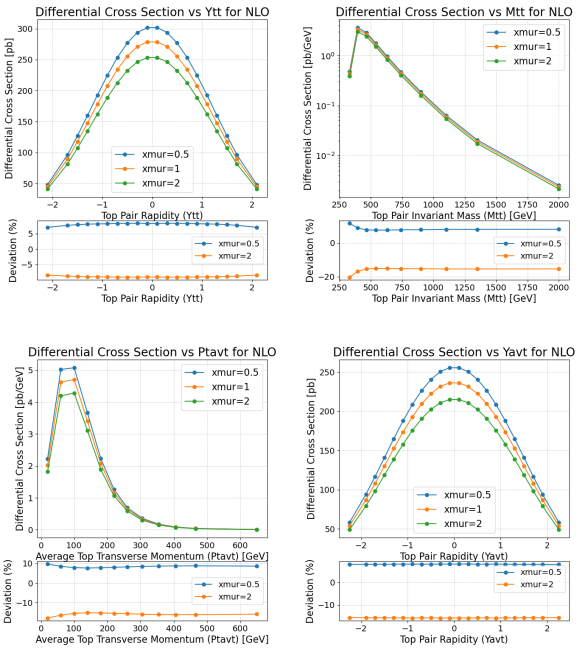

Figure 6: Differential Cross Section (NLO) as a function of the observables for 3 values of μ_R and the deviation from $\mu_R = 1$.

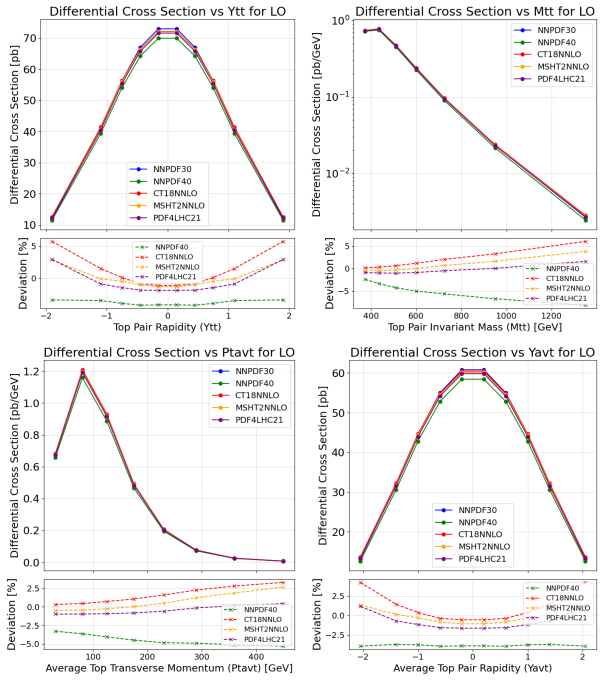

Figure 8: Differential Cross Section (LO) in function of the observables for different PDFs and the deviation from those PDFs and the NNPDF30 at $13TeV$.

and compared to the NNPDF30 set at 13 TeV. The resulting deviations, which illustrate the effect of different PDFs on the predictions, are shown in Figures 8, 9, and 10.

In contradiction to the results from the deviation of the μ_R, here the term of the perturbative expansion does not influence the deviation much.

For NNPDF40, we have an average deviation of -4%, CT18NNLO has a deviation of around

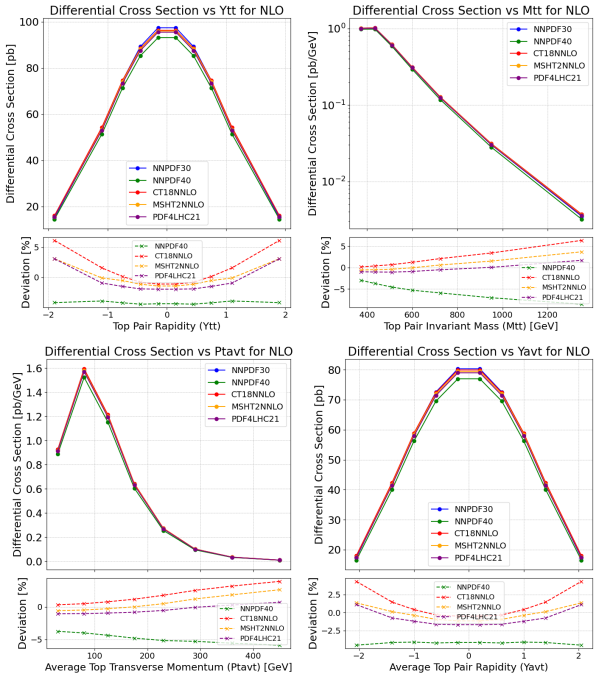

Figure 9: Differential Cross Section (NLO) in function of the observables for different PDFs and the deviation from those PDFs and the NNPDF30 at $13TeV$.

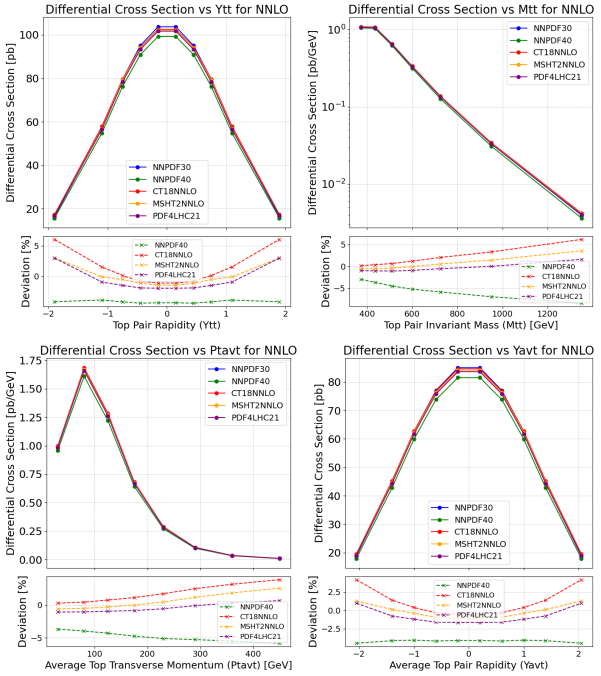

Figure 10: Differential Cross Section (NLO) in function of the observables for different PDFs and the deviation from those PDFs and the NNPDF30 at $13TeV$.

0.8%, MSHT2NNLO has a deviation of −0.3%, and PDF4LHC21 has a deviation of 0.9%.

4 Results and Conclusions

From the studies made, one can conclude that the perturbative expansion converges, since from the figures 3 and 4 the K-factor of the NNLO is smaller than the one for the NLO, which is very important because we always want our expansions to converge, so they can have a physical meaning.

The variation of μ_R shows that the renormalization scale has a strong influence on the differential cross section, particularly at $\mu_R = 2$. This sensitivity is reduced at NLO and is expected to diminish further at NNLO as higher-order corrections typically stabilize the prediction. In this analysis, however, the deviation increases again at NNLO, which is likely due to the interpolation grid from Ref. [3] lacking some of the necessary components to perform a consistent scale variation at this perturbative order. To clarify this behavior, additional investigations using Monte Carlo simulations will be required.

Now, for the variation of the PDF, one can note that the term of the expansion doesn't have a meaningful impact on the differential cross section, and the impact that the PDF used has on it is much smaller than that of the renormalization scale.

Acknowledgements

I would like to thank my supervisor and all the LIP community for their support in this project. In this internship, I learned a lot of important physics concepts and I deepened my knowledge about processing data using Python to access the data from the Excel, and also got familiarized with an important tool in this field, the fastNLO.

References

[1] *fastnlo: Fast pqcd calculations for pdf fits and phenomenology*, https://fastnlo.hepforge.org/, accessed: 2025-10-11

[2] *Lhapdf: The les houches accord parton density function interface*, https://www.lhapdf.org/, accessed: 2025-10-11

[3] *Precision top quark pair production at nnlo*, https://www.precision.hep.phy.cam.ac.uk/results/ttbar-fastnlo/, accessed: 2025-10-11